

Geology, mineralogy, and fluids inclusion studies in Shadan copper-gold deposit, Southern Khorasan

Parivash Mahdavi¹, Alireza Jafari-Rad^{1*}, Soraya Heuss-Abbichler², Mohamad Lotfi³, Nima Nezafati¹

¹ Department of Earth Sciences, Science and Research Branch, Islamic Azad University, Tehran, Iran

² Department of Earth and Environmental Sciences, Ludwig-Maximilians University of Munich, Germany

³ Research Institute for Earth Sciences, Geological Survey of Iran, Tehran, Iran

*Corresponding author, e-mail: alirad@yahoo.com

(received: 08/09/2019 ; accepted: 22/12/2019)

Abstract

Shadan copper-gold deposit is located in nearly 65km Southwest of Birjand. The area is a part of eastern margin tertiary volcano-plutonic belt in Lut Block. The oldest units in this area are tertiary andesite, tuff, rhyolite, and rhyolitic tuff. The units are intruded by late Eocene–Oligocene quartz monzonite-granodioritic (Shadan porphyry), granite, and granodiorite intrusion rocks. The rocks are again overlain by Quaternary deposits. Shadan deposit is considered as Cu-Au porphyry in which mineralization was controlled by tectonic structures. The deposit is hosted by dacite, rhyodacite and quartz monzonite and granodiorite rocks which are mainly associated with potassic, sericitic, argillic and propylitic alterations. Mineralization mostly occurs as disseminated, stockwork, veins and veinlets in the host rocks. The paragenesis in veins and veinlets includes quartz, pyrite, chalcopyrite, bornite, chalcocite, pyrrhotite, magnetite, hematite and covellite, gold, malachite and iron-hydroxides. Gold grains are between 1 to 150µm in diameter commonly occurring within the quartz and in some places occur in <10µm diameter within oxidized pyrites. Fluid inclusion studies on 5 types of fluids reveal that homogenization temperatures range between 150 and 500°C (Average 350°C) with salinity from 10 to 60wt.% NaCl equivalent. Field observation and laboratory studies suggested that the mineralization likely belongs to porphyry magmatic-hydrothermal systems.

Keywords: Shadan, Porphyry, Copper- Gold, Mineralogy, Fluid Inclusions.

Introduction

Porphyry copper systems are mainly developed at convergent plate margins, including continental margin and island-arc settings (Sillitoe, 2010), where the subduction of oceanic crust is related to arc-type magmatism that generates most of the hydrous, oxidized upper crustal granitoid genetically related to ores (Aghazadeh *et al.*, 2015). The evolution of the Neo-Tethys Ocean in Iran is associated with different kinds of mineralization and metal deposits including porphyry copper deposits (PCDs). The PCDs in Iran are placed in four belts: Arasbaran, the middle part of the Urumieh–Dokhtar Magmatic Arc (UDMA), Kerman, and East Iran, consist of Lut Block (Aghazadeh *et al.*, 2015). The Lut block is the main body of eastern Iran (Figs. 1 and 2). The present eastern border of the Lut Block would have belonged to the active margin of the subducted Neotethys Ocean (Dercourt *et al.*, 1994; Golonka, 2004; Bagheri & Stampfli, 2008). The volcanic–plutonic belt within the Lut Block extends in the N–S direction about 900 km (Figs. 1 and 2). This belt during Jurassic to Tertiary magmatism stages formed various mineralization types, such as Cu–Mo–Au porphyry- type deposits, epithermal-type ores, Cu–Au–Ag IOCG-type deposits, Cu and Au–

Sb–Pb–Zn vein-type deposits, Cu–Au massive sulfide-type deposits, granite related Sn–W–Au ores and skarn Sn deposits. (Malekzadeh, 2009; Arjmandzadeh *et al.*, 2011, 2014).

In this relation, known deposits in the northern part of the belt are including Shadan, Khupik, Maher Abad, Chah Zaghrou, Hired, Qaleh Zari and other small occurrences (Fig. 2). Shadan porphyry Cu–Au deposit is located about 65 km southwest of Birjand near the Khosf city in South Khorasan province. This deposit lies between longitude (E) 58.979720 and latitude (N) 32.357220 (Figs. 2 and 3). This deposit is one of the best Cu–Au porphyry resources in the east edge of the Lut block, east of Iran. The purpose of this work is to present and discuss fluid inclusion data from Shadan porphyry, aiming at establishing PVXT conditions and provide comprehensive information about evolution of the ore fluids.

Regional geological setting

Iran is a part of Alpine-Himalayan orogenic belt, which resulted from the disappearance of Neotethyan ocean (Dercourt *et al.*, 1993; Stampfli & Borel, 2002; Omrani, 2008) from Cretaceous and Tertiary convergence between the Eurasian and the Afro-Arabian plates (Berberian & King, 1981;

Mohajjel *et al.*, 2003; Agard *et al.*, 2011; Ghasemi & Talbot, 2006). Three major structural units can be distinguished in Iran (Berberian & King, 1981). They include the Zagros fold and thrust belt (southern unit), the central unit (Cimmerian block) and the northern unit (the Kopet Dagh Mountains).

The Cimmerian blocks of Iran are parts of the orogenic system in western Asia (Alpine-Himalayan) and consist of several continental blocks (Stöcklin, 1968) included of the Yazd, Tabas, and Lut blocks (Fig. 1).

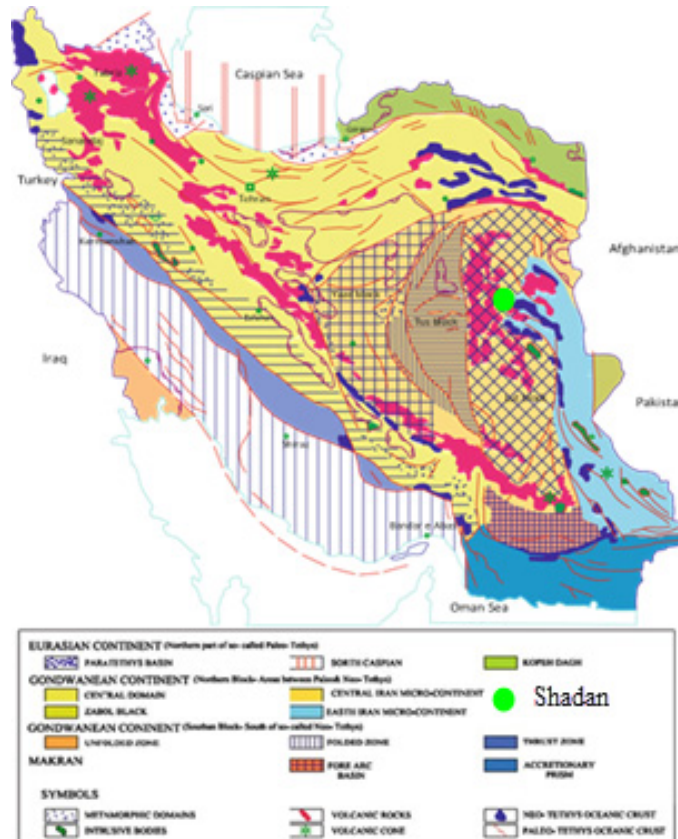


Figure 1. Important tectono-sedimentary areas of Iran (Aghanabati, 2004). The Cimmerian blocks as a part of Central Iran domain included of the Yazd, Tabas, and Lut blocks have shown in this figure.

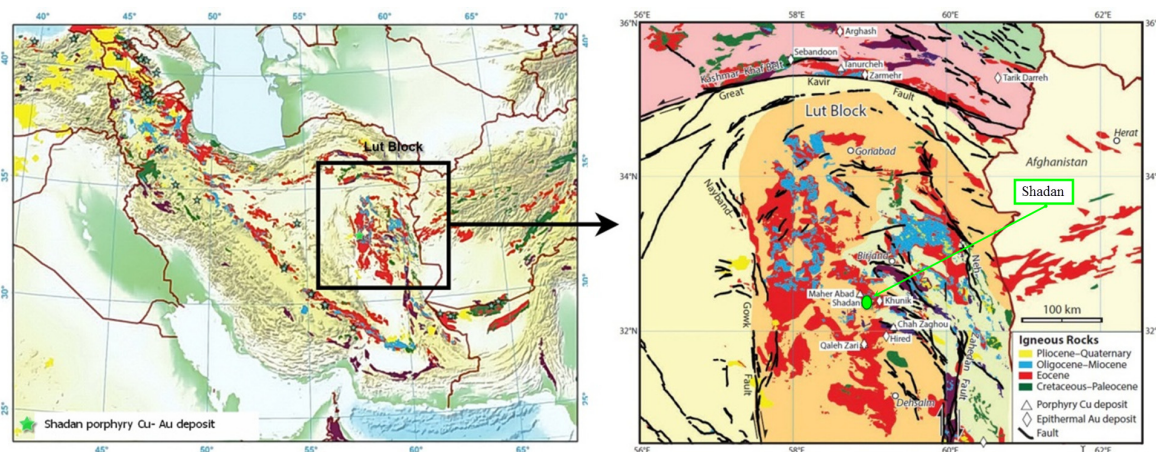


Figure 2. Main tectonic elements of Iran and neighboring countries, showing late Cenozoic and Cenozoic magmatism and the locations of major Shadan porphyry deposit. (Modified after Richards & Sholeh, 2016).

The Lut Block is one of several microcontinental blocks interpreted to have drifted from the northern margin of Gondwanaland during the Permian opening of the Neo-Tethys, which was subsequently accreted to the Eurasian continent in the Late Triassic during the closure of the Paleo-Tethys (Golonka, 2004). Eftekharnjad (1981) proposed that magmatism in the northern Lut area resulted from the subduction of Afghan Block beneath the Lut Block, and Berberian (1983) showed that igneous rocks at Lut Block had a calc-alkaline arc signature. Recently, asymmetric subduction models have been discussed for situations similar to that of the Lut Block (Arjmandzadeh *et al.*, 2011, 2014; Doglioni *et al.*, 2009). The Lut Block extends some 900 km from the Doruneh Fault in the north to the Jazmorian basin in the south and is ~ 200 km wide (Stocklin & Nabavi, 1973). The Lut Block consists of a pre-Jurassic metamorphic basement, Jurassic sedimentary rocks and several generations of Late Mesozoic and Cenozoic intrusive and/or volcanic rocks (Fig. 2) (Camp & Griffis, 1982; Tirrul *et al.*, 1983). Radiometric age data indicate that the oldest magmatic activity in the central Lut Block took place

in the Jurassic (Tarkian *et al.*, 1983). Further to the north, magmatic activity started in Upper Cretaceous (75 Ma) and generated both volcanic and intrusive rocks (Tarkian *et al.*, 1983). The Middle Eocene (47 Ma) was characterized by alkaline and shoshonitic volcanism with a peak at the end of the Eocene. In addition, calc-alkaline basalts and basaltic andesites erupted in the Eocene-Oligocene (40–31 Ma) (Tarkian *et al.*, 1983).

The Shadan porphyry Cu - Au deposit, the most mineralized zones are concentrated in a 1.5-km² area and were mapped at a 1:1,000 scale (Karand Saderjahan, 2015). These detailed maps are shown in Fig. 3. This area is a part of Lut block with N-S trend. The rocks in the vicinity of the Shadan deposit predominantly consist of Eocene-Oligocene intermediate to acidic lava flows as andesite, rhyolite, and rhyolitic tuff, tuff and felsic subvolcanic as a granodiorite and quartz monzonite. Granodiorite and quartz monzonite are the specific host rocks for the copper and gold mineralization. The local stratigraphy, from oldest to youngest in the Shadan area, includes the following (Fig 3):

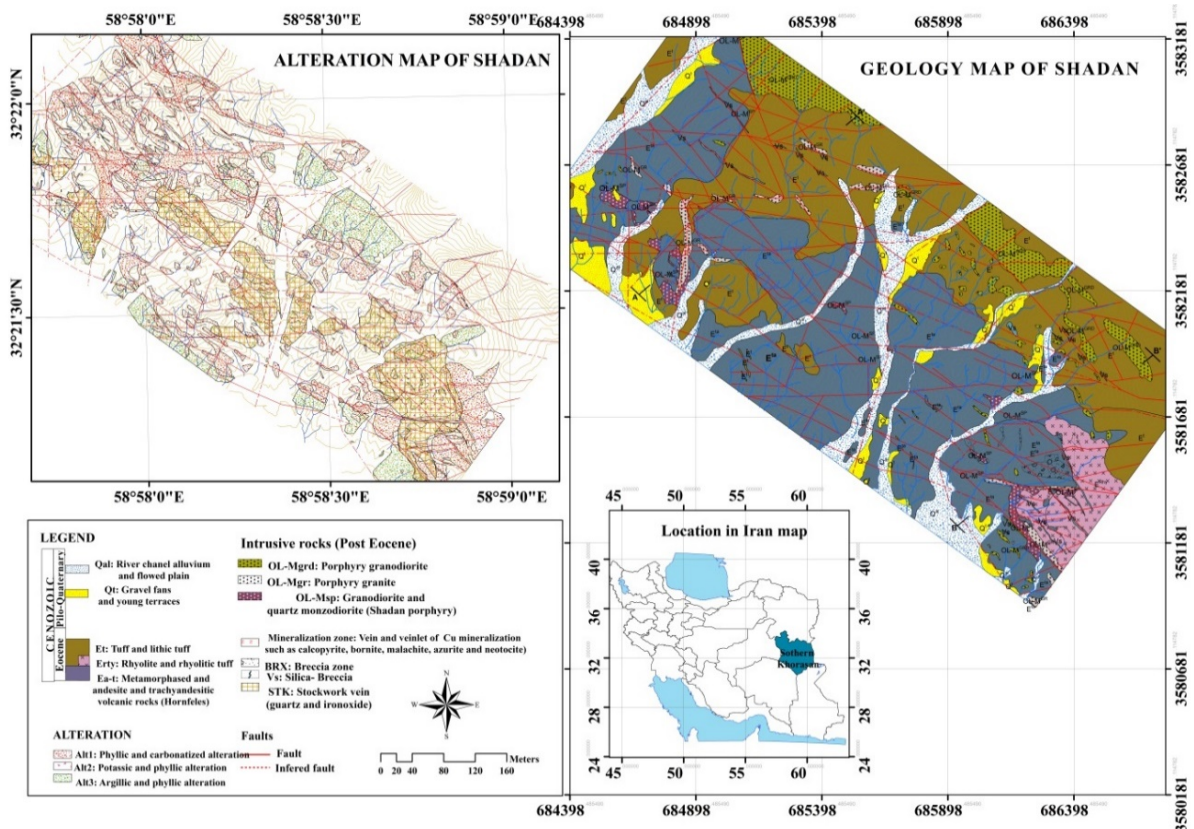


Figure 3. Local geological and alteration map at the Shadan deposit mapped at a scale of 1:1,000 (Karand Sadrejahjan Co, 2015).

1. A sequence of thin-bedded green andesite ($E_2^{1.1}$) composition that are extensively altered in the vicinity of the younger intrusive rock. In marginal parts of the study area, due to proximity intrusive units, andesitic rocks have been changed to hornfels. This unit has shown potassic, phyllic and also argillic alterations. Some part of this andesitic unit has been mineralized.

2. Gray to green tuffs, lapilli tuff and breccia tuff, volcanic breccias, and intermediate lava flows with the andesitic (E^1) composition of middle Eocene age. This unit outcropped in the eastern part of the Shadan area and directly located on andesitic unit.

3. Rhyolite and rhyolitic tuff (E^{th}). This unit exposed in southern and southeastern parts of the study area which is gradually (transitionally) changed to tuff unit. This unit contains porphyritic texture with feldspar (plagioclase and sanidine) and also quartz phenocrysts. In marginal parts of Shadan porphyry intrusive, siliceous stockworks observed. Also, Potassic and quartz sericite alteration observed in marginal part of this unit.

4. Subvolcanic granodiorite, quartz monzonite plutons (Pgd) and dikes have intruded into the above volcanic sequence during Oligocene. In this area, they are oldest fertilized intrusive units which is called Shadan porphyry. In the eastern part of the area, this unit observed in three separated shape as stock, apophysis and sometimes dyke.

5. The youngest rock unit in the studied area is Granodioritic (Gd). This unit is found as stock, dyke, and apophysis in eastern and southern parts of the Shadan area. This body is barren and it is usually is fresh. According to the geochemical diagrams, the rocks of the study area mostly high K calc-alkalic in composition

6. Finally, Quaternary deposits (Q^{al} and Q^1) overlined the oldest rocks unit and have been developed in western and southwestern parts of Shadan area (Karand Saderjahan, 2015).

Structurally, in this area, there are three fracture and fault systems with NW-SE (N50W), E-W and NE-SW (N50_70E) trends. NW-SE fracture system is a major system and it is followed by other systems. In the Shadan area, NW_SE faulting system plays as a main role in emplacing intrusive body and also mineralization (Karand Sadrejahān, 2014).

Method

More than 140 polished and thin sections were prepared from the volcano- plutonic rock samples collected from surface and boreholes at the Shadan

deposit for mineralogical and petrographic studies 48 doubly polished wafers prepared for fluid inclusion studies were examined petrographically. Doubly polished wafers were prepared using the procedure of Shepherd *et al.*, 1985. The thickness of the wafers varied between 80 and 200 μm , depending upon the transparency of the quartz crystals. Sample selection was biased to quartz containing an abundance ore-related sulfide minerals. 32 wafers containing suitable fluid inclusions from quartz were selected for microthermometric measurements. The measurements. Measurements were made using a Linkam THMSG 600 combined heating and freezing stage with a temperature range of -196°C to 600°C , mounted on a Nikon petrographic microscope. These studies carried out in Karaj mineral research and processing center laboratory. The system was calibrated with inorganic standards by using N-Hexan with -94.3°C as melting point and Cesium nitrate with 414°C as melting point. Calibration error is up to $\pm 0.2^\circ\text{C}$. and $\pm 0.6^\circ\text{C}$ for N-Hexan and Cesium nitrate respectively. To avoid decrepitation of the inclusions, freezing was carried out prior to heating.

Discussion

Mineralization and alteration

As noted above, in the Shadan porphyry Cu-Au deposit mineralized zones were mapped at a 1:1,000 scale (Karand Saderjahan, 2015). Based on Field and microscopic studies styles of mineralization include disseminated, stockwork, hydrothermal breccia, veins, and veinlets. Stockwork ore is the most relevant type and is mainly found in the western part of area. Mineralization in Shadan area occurred in two distinct zones; respectively oxide and sulfide zones. Principal metallic minerals in these zones include pyrite, chalcopyrite, chalcocite, bornite, magnetite, pyrrhotite, hematite, covellite, malachite, Fe-hydroxides (Fig. 4).

Principal non-metallic minerals as a gangue mineral include quartz (over 70%), plagioclase, muscovite and less than biotite, calcite, pyroxene, and olivine. Mineralogically and spatially different alterations have affected the volcano-plutonic units in the Shadan deposit area consist of potassic, phyllic, propylitic, argillic, silicification and tourmalinitization types (Fig. 5). The first alteration in the subvolcanic intrusions host rocks of mineralization is a potassic alteration. Mineralogy of this extensive alteration includes feldspar, kaolinite, and quartz. This alteration can be clearly

observed by anhedral biotite, magnetite and vein-veinlet orthoclase (Fig. 6a). Phyllic alteration is determined by quartz, sericite and sometimes pyrite(Fig. 6b). In this alteration, copper mineralization occurred as the primary sulfide. Propylitic alteration widely extends in the study area and defined by anhydrite, chlorite, and epidote

(Fig. 6c). Finally, the argillic alteration with white to bright gray - cream color observed in around of propylitic alteration. This alteration is determined by clay minerals especially montmorillonite, kaolinite, and alunite. Also, tourmalinization observed in a restricted area around the silicification in Shadan porphyry system (Fig. 6d).

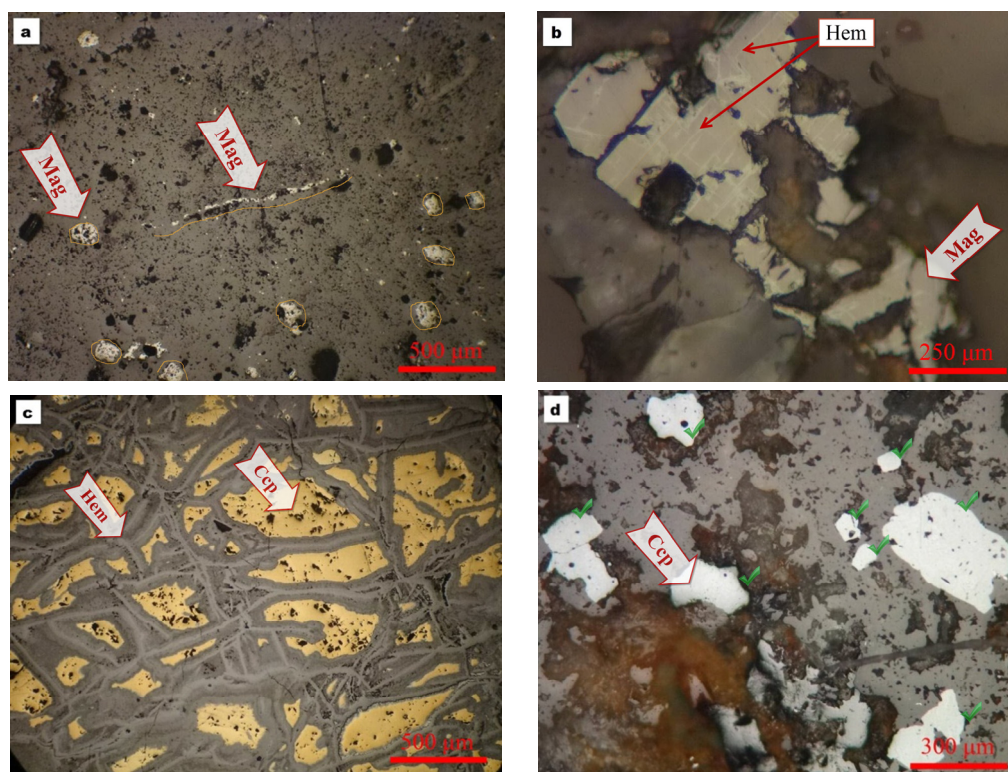


Figure 4. (a) Distribution of magnetite in veinlet and scattered in the sample, (b) magnetite with martitization along the octahedral planes replaced by hematite. (c) Chalcopyrite as vein and veinlet replaced by hematite (d) newly formed chalcopyrite distributed in sample (Ccp:Chalcopyrite, Hem:Hematite, Mag:magnetite).

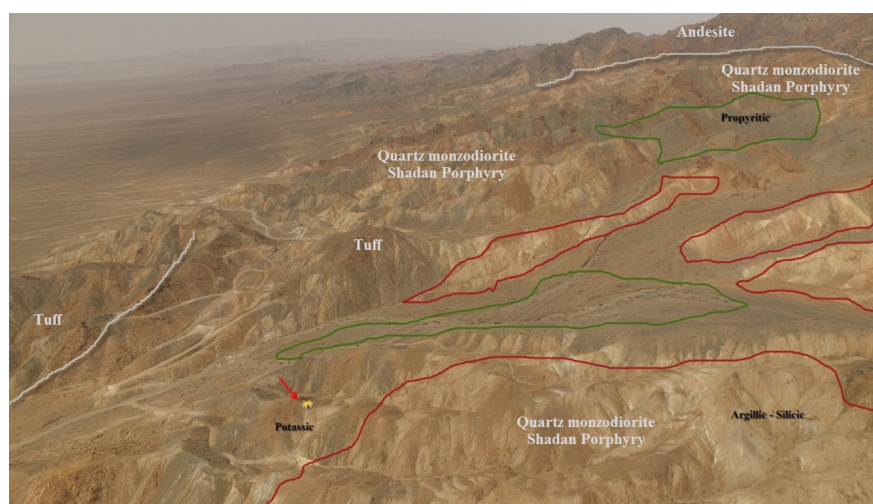


Figure 5. View to the north from Shadan area, Intensive argillic-siliceous alterations of the bedrock (red border) and local areas with propylitic(green border) and potassic alterations(star).

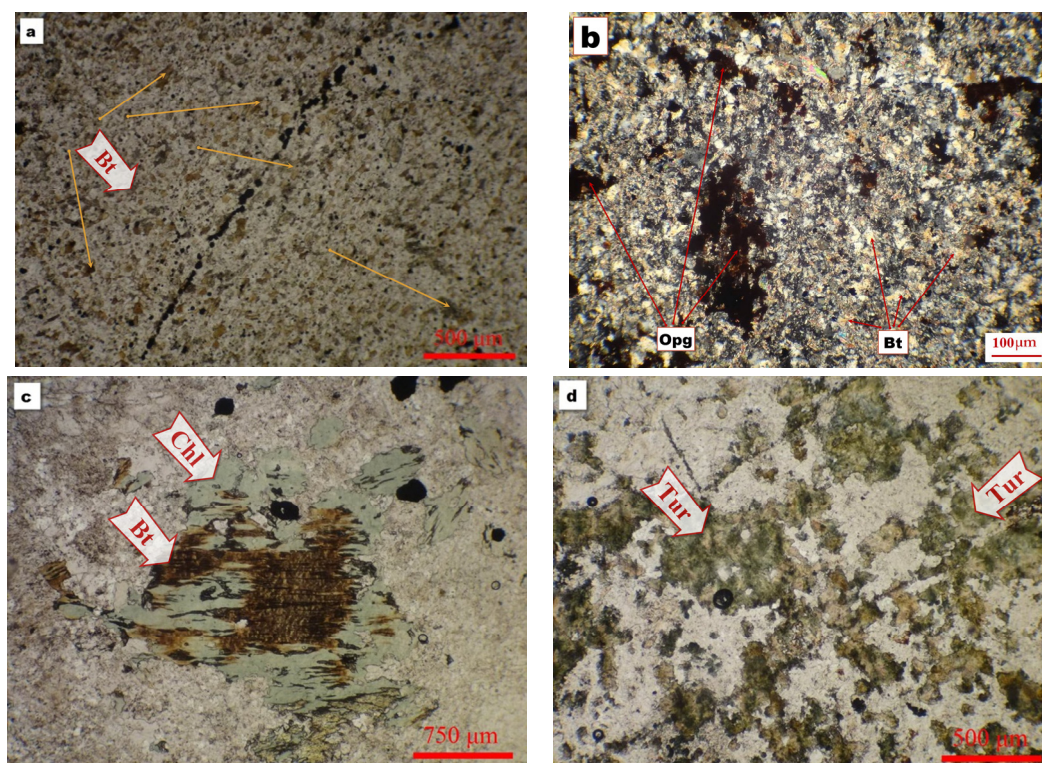


Figure 6. Thin sections showing (a) Hornfelsic tuff with potassic alteration including secondary biotite and veinlet containing opaque minerals, normal light (b) Sample with phyllitic alteration with abundant quartz and sericite, polarized light (c) Porphyry granodiorite with propylitic alteration, including replacement of biotite phenocryst by chlorite and epidote, normal light (d) Trachyandesite with widespread tourmalinization, normal light (Bt:biotite, Chl:Clorite, Tur:Tourmaline, Opg:Opaque mineral).

Petrography of fluid inclusion

The morphology and petrographic characteristics of the fluid inclusions were recorded at room temperature using the criteria of Roedder (1984) and Shepherd *et al.*, (1985). Furthermore, the liquid/vapor phase ratios were estimated with the aid of standardized charts (Shepherd *et al.*, 1985). The inclusions were classified on the basis of host mineral occurrence, their relationship to each other, and the type of inclusion. With respect to their relationship to the host mineral, they are classified as primary (isolated inclusions, as well as those in growth zones), secondary (inclusions occurring along with fractures that intersect the crystallographic surfaces), and pseudo-secondary (inclusions occurring along fractures that do not intersect the crystallographic surfaces). Secondary and necked inclusions were avoided during microthermometric analysis. Fifteen quartz vein samples from outcrop and drill cores were selected for microthermometric measurements. In sample selection, care was taken to prepare quartz grains typically in sulfide-gold pressure shadows and to select fluid inclusion assemblages deemed related to

mineralization for microthermometric measurement. In addition, to minimize the effect of post-entrapment modifications such as necking down, partial or total leakage, and selective leaching or diffusion of some components, inclusions suspected to have been affected by such modifications were clearly avoided. All microthermometric measurements were carried out on ore stage quartz samples. Data were mostly obtained from inclusions ranging up to 35 μm in size, but mostly as large as 10 μm . Fluid inclusions in quartz have a different shape, but irregular, flat, spherical and ellipsoid shapes are dominated.

Based on the number of phases present at room temperature and their microthermometric behavior, five fluid inclusion types were recognized. Type I inclusions contain a one-phase liquid at room temperature (Fig. 7h). These inclusions may be irregular, rounded, or rectangular in shape. The size of the inclusions varies between 5 and 18 μm . Type II inclusions (Fig. 7g) are vapor rich groups. Optically, the vapor phase occupies the entire volume of the inclusion in the vapor-rich group, although as much as 50 vol. % liquid enclosing the vapor phase

may go undetected in such inclusions. Type III aqueous inclusions contain two phases at room temperature. These type of inclusions divided into two groups one set are liquid-rich (IIIA) and contain two phases at room temperature with the bubble

occupying 40 to 50% of the total inclusion volume and other set are vapor rich (IIIB) and contain two phases at room temperature with the bubble occupying 60 to 90% of the total inclusion volume.

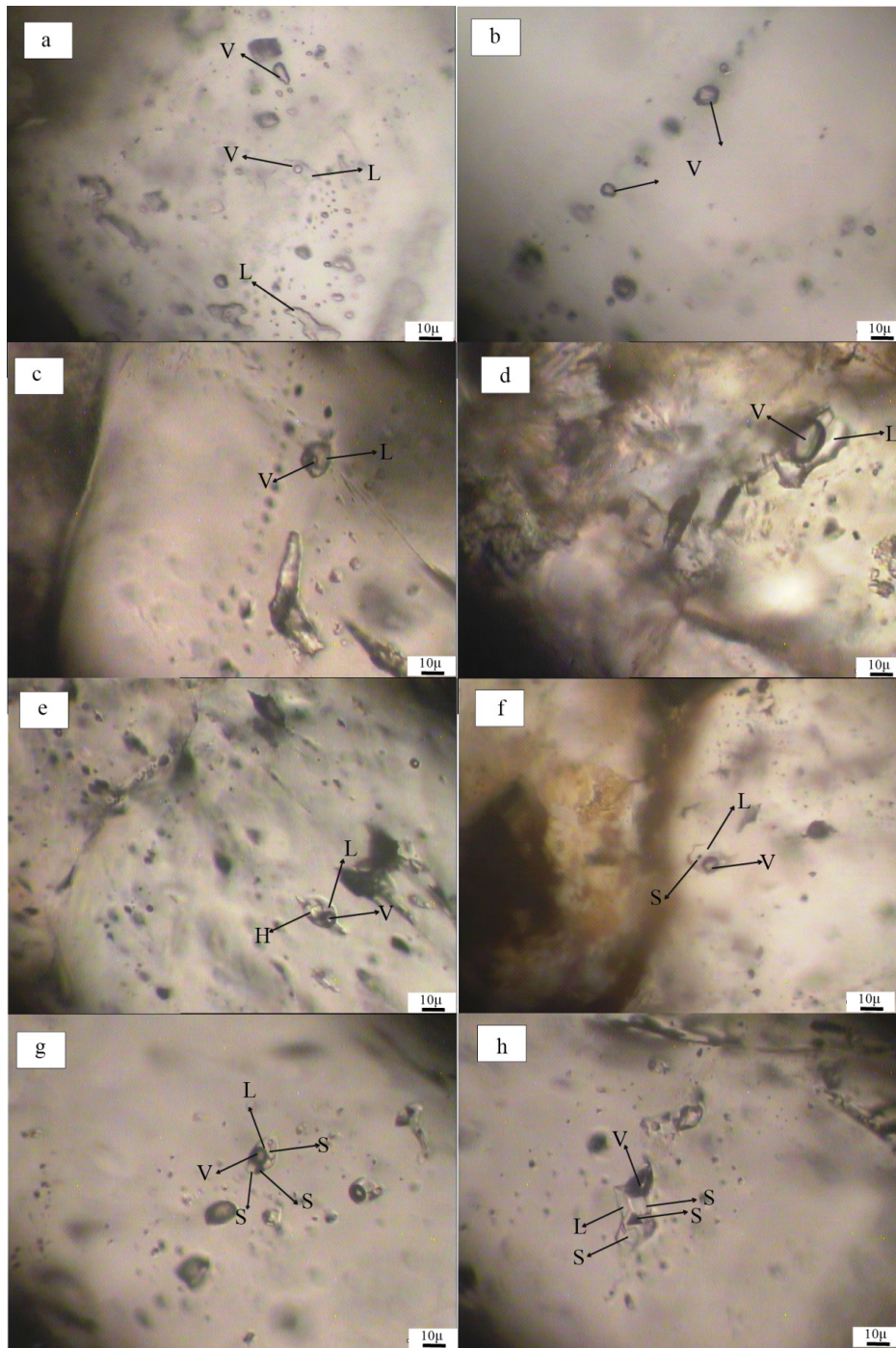


Figure 7. Microscopic images of fluid inclusions in quartz mineral of Shadan ore. a, b) A collection of multi-phase brine involved fluids. c) Simple brine involved fluids. d) Three-phase involved fluids with solid phase. e) Two-phase involved fluid enriched by liquid. f) Two-phase enriched by gas. g) Monophase (gas). h) A collection of mono-phase (gas) and (liquid) with two-phase enriched by liquid.

Both types of these inclusions are faceted, rounded and subrounded, with sizes generally less than 25 μm . These inclusions appear as isolated cavities or as clusters and in arrays and are recognized by transparency and low relief. (Fig. 7e, f).

Type IV inclusions (Fig. 7c, d) contain three-phase liquid, solid and gas (aqueous liquid + vapor + halite \pm sylvite) at room temperature. The three-phase inclusions contain a small vapor bubble at room temperature, filling 30 to 40% of the total inclusion volume. These inclusions are faceted to subrounded and may reach 20 μm in size. Type IV inclusions commonly occur as sets of spread planar arrays, restricted to the interiors of quartz grains. Type V inclusions contain three-phase liquid, multi solid, and gas (aqueous liquid + vapor + halite \pm sylvite + opaque minerals). These type of fluid inclusions are relatively common and mostly occurred as irregular shape (Fig. 7a, b).

Micro-thermometry results

Collected fluid inclusion data included temperatures of total homogenization (TH total), first ice melting (TFM), and final ice melting (TM) for aqueous inclusions.

In the multiphase solid inclusions, two points were recorded: (1) TH (NaCl) (the temperature at which halite dissolves) and (2) TH (LV) (the temperature of vapor and liquid homogenization).

Microthermometric measurement data and volume fraction estimates of the different phases were processed utilizing the program packages FLUIDS (Bakker, 2008). Salinities were estimated after (Bodnar, 1994) from TMice, for aqueous inclusions. The salinities of multiphase bearing fluid inclusions were calculated using the dissolution temperatures of daughter minerals (Hall et al., 1988). Because the opaque daughter minerals do not melt during the heating process, the salinities presented here do not include the contribution of these opaque daughter minerals. Densities of H₂O and NaCl fluid inclusions are calculated from the equation of state by Zhang and Frantz (1987) and Holloway (1981) respectively.

For the isochore calculations, we used the program FLINCOR (Brown, 1989). In addition, we used the equation states of H₂O in P–T projection (Diamond, 2003) for pressure estimate in two-phase aqueous inclusions. Microthermometric measurements for about 210 primary fluid inclusions. The results from micro-thermometry on different kinds of involved fluids have been shown in (Figs. 8a, b).

The average TH, to a liquid or vapor, of type III primary inclusions in quartz range from 236°C to 335°C for various studied fluid inclusion assemblages. The salinities of type III fluid inclusions ranges are between 10.49 and 16.15 wt. % NaCl equiv.

The homogenization temperatures (TH) of the IV type of primary inclusions in vary between 330°C and 460°C (mean: 420°C) based on daughter halite dissolved, corresponding to high salinities of 28–65 wt.% NaCl equivalent. These hypersaline fluid inclusions are totally homogenized to liquid.

In The fluid inclusions type V, opaque minerals do not melt in heating runs, while the daughter halite and sylvite dissolved at 330°C to 490°C (T_m Na-KCl), corresponding to high salinities of 37- 45 wt.% NaCl equivalent for halite and 28.9–32.5 for sylvite.

Estimates of trapping pressures for ore-forming fluids were determined using inclusion types III and IV and the methodology described by (Touret & Dietvorst, 1983). Also, we estimated the trapping pressures using the Flincor program (Brown, 1989) for the H₂O–NaCl system.

The homogenization temperatures of the type-II fluid inclusions in vary between 235°C and 335°C. The trapping pressure of the fluid inclusions was estimated to be 95.7 to 142.1 MPa, which corresponds to a depth of 2850 to 4000 m (assuming a constant pressure gradient of ~29.4 MPa per 1 km of depth).

Density variation is shown in Fig. 8c. Their fluid inclusions demonstrate that the density varies from 0.7 to ~1.5 g/cm³, but the range of 1.1 to 1.3 g/cm³ show the highest frequency of densities for the fluids.

Coexisting liquid-rich and vapor-rich inclusions and assemblages of vapor-rich only inclusions are observed in the studied samples which could imply boiling conditions at the time of entrapment. Fluid boiling, cooling and early magmatic mixture with meteoric waters may have led to mineralization (Wilkinson, 2001). Fluid inclusion evidence shows cooling effect, mixture with meteoric water; boiling and formation of solutions with high salinity and density of the ore-forming fluids (Figs. 8d, e).

The high trapping temperatures and high salinity of type IV and V fluid inclusions suggest that fluid population probably represents an orthomagmatic fluid which is exsolved as a high-density phase from Shadan granodiorite and subsequently saturated with halite and boiled. We suggest that the

source of fluid III was also mainly orthomagmatic (high salinity), but it circulated at a lower temperature than fluid type IV and V and mixed with external meteoric water. This is also suggested by a trend from higher temperature and higher

salinity to lower temperature and lower salinity for III and IV fluid inclusions. Coexistence of fluid inclusions type I with III indicates that boiling extensively.

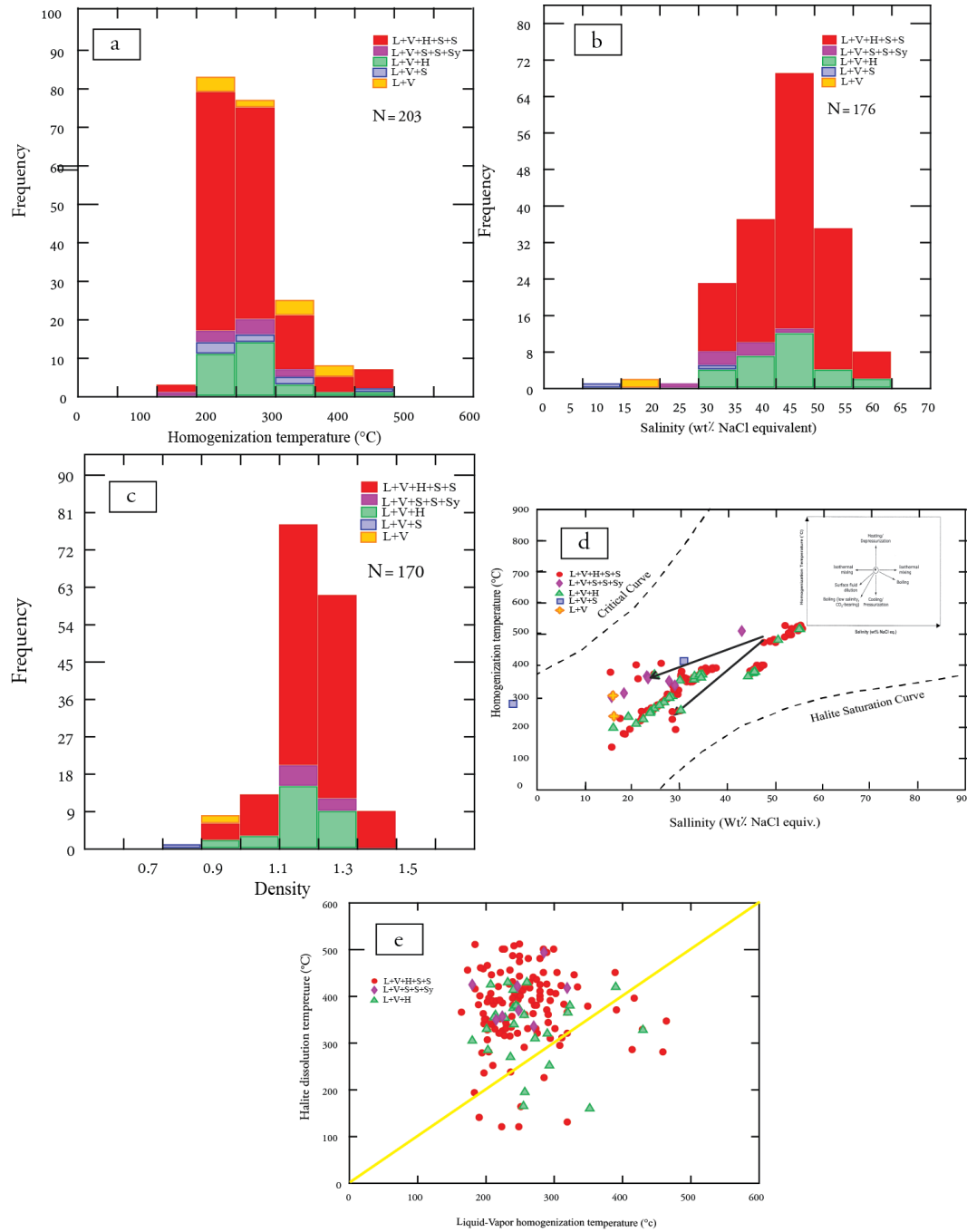


Figure 8. Results of the micro- thermometry of the different types of fluid inclusions measured in quartz mineral of Shadan deposit: Histogram of a) homogenization temperature (Th), b) salinity, c) density of fluid inclusions, d) diagram of homogenization temperature versus salinity in order to define mineralization environment, e) temperature of homogenizing liquid to gas versus halite solution in multi-phase involved fluids.

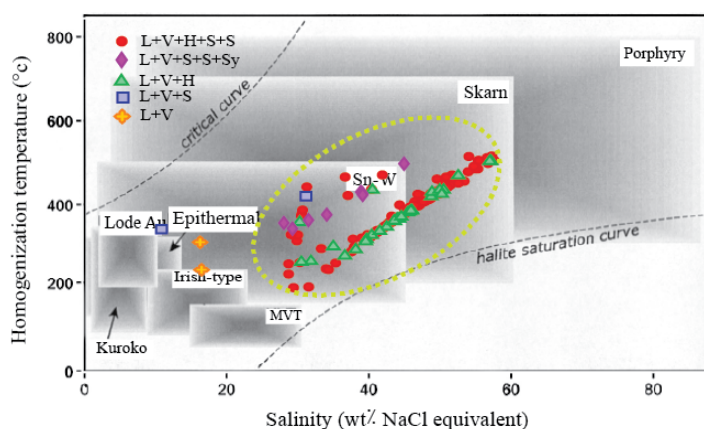


Figure 9. The Th vs. salinity plot (Wilkinson, 2001) for fluid inclusion data of Shadan deposits.

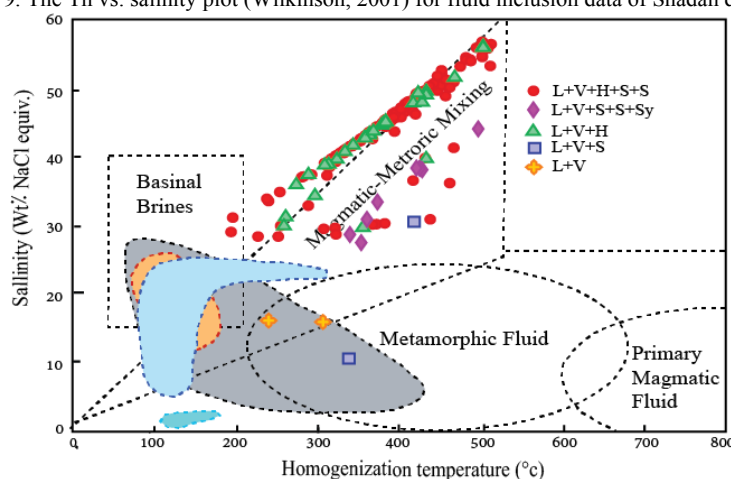


Figure 10. The Th vs. salinity plot (Beane, 1983) for fluid inclusion data of Shadan porphyry deposits.

Conclusion

Shadan deposit formed during Tertiary continental collision between the Afghan and Iranian plates. The mineralization is controlled by structures. The ore-bearing units are generally Eocene calc-alkaline subvolcanic intrusive stocks exposed along a northwest to southeast oriented trends in the eastern part of the Lut Block, eastern Iran. The deposit was found within extensional fractures occur as a disseminated, stockwork, and minor hydrothermal breccia styles as veins and veinlets. Extensive hydrothermal alteration includes potassic, phyllic, propylitic, argillic, silicification and tourmalinitization types within host Shadan subvolcanic and volcanic around observed in this area. Mineralization took place in being economically important in terms of base metal,

precious and iron mineralization, including quartz, pyrite, chalcopyrite, chalcocite, bornite, magnetite, covellite, malachite, Fe-hydroxide and native gold.

Fluid inclusion studies on 5 types of fluids reveal that homogenization temperatures range between 300- 500°C (Average 360°C) with salinity from 10 to 60 wt.% NaCl equivalent (Average 40 wt.% NaCl) that indicate high contents of NaCl- KCl in ore fluid.

Salinity vs. homogenization temperature plot for the fluid inclusion data at Shadan shows that the fluid inclusions plot on the porphyry fields (Figs. 9 and 10).

Based on geology, alteration styles, mineralization types and fluid inclusion the Shadan deposit it's belongs to the porphyry copper deposits.

References

- Agard, P., Omrani, J., Jolivet, L., Mouthereau, F., 2005. Convergence history across Zagros (Iran): Constraints from collisional and earlier deformation. *International Journal of Earth Sciences*, 94: 401–419.
- Agard, P., Omrani, J., Jolivet, L., Whitechurch, H., Vrielynck, B., Spakman, W., Monie, P., Meyer, B., Wortel, R., 2011.

- Zagros orogeny: a subduction-dominated process. *Geological Magazine*, 148: 692–725.
- Aghanabati, A., 2004. Geological of Iran, Geological Survey of Iran, 606 pp. (in Persian). *J. Iran. Pet. Soc.*
- Aghazadeh, M., Hou, Z., Badrzadeh, Z. and Zhou, L., 2015. Temporal–spatial distribution and tectonic setting of porphyry copper deposits in Iran: constraints from zircon U–Pb and molybdenite Re–Os geochronology. *Ore geology reviews*, 70: 385–406.
- Arjmandzadeh, R., 2011. Mineralization, geochemistry, geochronology, and determination of tectonomagmatic setting of intrusive rocks in Dehsalm and Chahshaljami prospect areas, Lut block, east of Iran. Ph.D. thesis, Ferdowsi University of Mashhad, 215 pp. (in Persian).
- Arjmandzadeh, R., Karimpour, M.H., Mazaheri, S.A., Santos, J.F., Medina, J.M., Homam, S.M., 2011. Sr–Nd isotope geochemistry and petrogenesis of the Chah-Shaljami granitoids (Lut block, eastern Iran). *Journal of Asian Earth Sciences*, 41: 283–296.
- Arjmandzadeh, R. and Santos, J.F., 2014. Sr–Nd isotope geochemistry and tectonomagmatic setting of the Dehsalm Cu–Mo porphyry mineralizing intrusives from Lut Block, eastern Iran. *International Journal of Earth Sciences*, 103(1), pp.123–140.
- Bagheri, S., Stampfli, G.M., 2008. The Anarak, Jandaq and Posht-e-Badam metamorphic complexes in central Iran: New geological data, relationships and tectonic implications. *Tectonophysics* 451:123–155. doi:10.1016/j.tecto.2007.11.047
- Bakker, R.J., 2008. AqSoVir software package fluids, v.2. Fluid inclusion laboratory Leoben, for fluid system: H₂O–NaCl–KCl–CaCl₂ (partly). <http://fluids.unileoben.ac.at/computer.html>.
- Bakker, R.J., 2008. Loner Ap software package fluids, v.2. Fluid inclusion laboratory Leoben, for fluid system: H₂O–CO₂–CH₄–NaCl–KCl. <http://fluids.unileoben.ac.at/computer.html>.
- Beane, R.E., 1983. The magmatic-meteoric transition. *Geothermal Resources Council*, 13: 245–253.
- Becker, S.P., Fall, A., Bodnar, R.J., 2011. Synthetic fluid inclusions. XVII. PVTX properties of high salinity H₂O–NaCl solutions (>30 wt% NaCl): application to fluid inclusions that homogenize by halite disappearance from porphyry copper and other hydrothermal ore deposits. *Economic Geology*, 103: 539–554.
- Berberian, M., 1981. Active faulting and tectonics of Iran. In: Gupta, H.K., Delany, F.M (Eds.), *Zagros Hindu Kush Himalaya Geodynamic Evolution*, vol. 3. American Geophysical Union, pp. 33–69.
- Berberian, M., 1983. Structural Evolution of the Iranian Plateau; Contribution to the Seismotectonics of Iran, Part IV: Continental Deformation in the Iranian Plateau. Geological Survey of Iran, Report 52: 19–68.
- Berberian, M., King, G.C.P., 1981. Towards paleogeography and tectonic evolution of Iran. *Canadian Journal of Earth Sciences*, 18: 210–265.
- Bodnar, R.J., 1983. A method of calculating fluid inclusions volumes based on vapor bubble diameters and P–V–T–X properties of inclusion fluids. *Economic Geology*, 78: 535–542.
- Bodnar, R.J., 1993. Revised equation and table for determining the freezing point depression of H₂O–NaCl solutions. *Geochimica et Cosmochimica Acta*, 57: 683–684.
- Bonder, R.J., Beane, R.E., 1980. Thermoporal and spatial variation in hydrothermal fluid characteristic during vein filling in preore cover overlying deeply buried porphyry copper-type mineralization at Red mountain, Arizona. *Economic Geology*, 75: 876–893.
- Bodnar, R.J., Vityk, M.O., 1994. Interpretation of microthermometric data for H₂O–NaCl fluid inclusions. Short course on fluid inclusions in minerals; Fluid inclusions in minerals, Pontignano, Italy, pp. 117–130.
- Brown, P.E., Lamb, W.M., 1989. P–V–T properties of fluids in the system H₂O–CO₂–NaCl: New graphical presentations and implications for fluid inclusion studies. *Geochimica et Cosmochimica Acta*, 53: 1209–1221.
- Camp, V., Griffis, R., 1982. Character, genesis and tectonic setting of igneous rocks in the Sistan suture zone, eastern Iran. *Lithos*, 15: 221–239.
- Cline, J.S., Bodnar, R.J., 1994. Direct evolution of brine from a crystallizing silicic melt at the Questa, New Mexico, molybdenum deposit. *Economic Geology*, 89: 1780–1802.
- Dercourt, J., Fourcade, E., Cecca, F., Azéma, J., Enay, R., Bassoulet, J. P., and Cottreau, N., 1994. Palaeoenvironment of the Jurassic system in the Western and Central Tethys (Toarcian, Callovian, Kimmeridgian, Tithonian): An overview. *Geobios*, 27, 625–644.
- Dercourt, J., Gaetani M, Vrielynck B, Barrier E, Biju-Duval B, Brunet M-F, Cadet JP, Crasquin S, Sandulescu M (eds) .,2000. Atlas Peri-Tethys Paleogeographical Maps, vol I–XX. CCGM/ CGMW, Paris, pp 1–269. 24 maps and explanatory note
- Dercourt, J., Zonenshain, L.P., Ricou, L.-E., Kazmin, V.G., Le Pichon, X., Knipper, A.L., Grandjacquet, C., Sbertshikov, I.M., Geysant, J., Lepvrier, C., Pechersky, D.H., Boulin, J., Sibuet, J.-C., Savostin, L.A., Sorokhtin, O., Westphal, M., Bazhenov, M.L., Lauer, J.P., and Biju-Duval, B., 1986. Geological evolution of the Tethys belt from the Atlantic to the Pamirs since the LIAS: *Tectonophysics*, 123: 241–315.
- Diamond, L.W., 2003. Glossary: Terms and Symbols used in Fluid Inclusion Studies, In: Samson, I., Anderson, A., Marshall, D (Eds.), *Fluid Inclusions, Analysis and Interpretation*, Short Course 32, Mineralogical Association of

- Canada, pp. 365–374.
- Dilles, J.H., Einaudi, M.T., 1992, Wall-rock alteration and hydrothermal flow paths about the Ann Mason porphyry copper deposit, Nevada, A 6-km vertical reconstruction. *Economic Geology*, 87: 1963–2001.
- Dogliani, C., Tonarini, S., Innocenti, F., 2009. Mantle wedge asymmetries and geochemical signatures along W- and E-NE directed subduction zones. *Lithos*, 113: 179–189.
- Eftekharnjad, J., Stockline, G., 1972, Geological map of Sarchahshour, 1:100 000. Geological Survey of Iran. (in Persian).
- Eftekharnjad, J., 1981. Tectonic division of Iran with respect to sedimentary basins. *Journal of Iranian Petroleum Society*, 82:19-28.
- Ghasemi, A., Talbot, C.J., 2006. A new tectonic scenario for the Sanandaj-Sirjan zone (Iran). *Journal of Asian Earth Sciences*, 26: 683–693.
- Golonka, J., 2004. Plate tectonic evolution of the southern margin of Eurasia in the Mesozoic and Cenozoic. *Tectonophysics*, 38: 235–273.
- Hall, D. L., Sterner, S. M., and Bodnar, R. J., 1988. Freezing point depression of NaCl-KCl-H₂O solutions. *Economic Geology*, 83(1): 197–202.
- Hitzman, M.W., 2000. Iron oxide-Cu-Au deposits: what, where, when and why. Hydrothermal iron-oxide copper-gold and related deposits: a global perspective, *Proceeding of AMF International Conference*, Adelaide, Australia, pp. 9–25.
- Holloway JR., 1981. Composition and volumes of supercritical fluids in the Earth crust. In: Hollister LS, Crawford ML (eds) *Fluid inclusions: applications to petrology*. Mineralogical Association of Canada Short Course Handbook 6, pp 13–38
- Karand Saderjahan Co., 2007. Geological map of Shadan exploratory area, scale 1:5000.
- Karand Saderjahan Co., 2015, Geological map of Shadan exploratory area, scale 1:1000.
- Karand Saderjahan Co., 2015, Report on completing exploratory operations in Shadan ore, 394 pp. (in Persian).
- Lecumberri-Sanchez, P., Steele-MacInnis, M., Bodnar, R.J., 2012. A numerical model to estimate trapping conditions of fluid inclusions that homogenize by halite disappearance. *Geochimica et Cosmochimica Acta*, 92: 14-22.
- Malekzadeh Shafaroudi, A., 2009. Geology, mineralization, alteration, geochemistry, microthermometry, radiogenic isotopes, petrogenesis of intrusive rocks and determination of source of mineralization in Maherabad and Khopik prospect areas, South Khorasan province. Ph.D. thesis, Ferdowsi University of Mashhad, 536 pp. (in Persian).
- Mohajjel M., Fergusson CL., Sahandi MR., 2003. Cretaceous–Tertiary convergence and continental collision, Sanandaj–Sirjan Zone, western Iran. *J Asian Earth Sci* 21:397–412
- Nabavi, M.H., 1976. An introduction to geology of Iran. (in Persian).
- Omrani J., 2008. The geodynamic evolution of Zagros: tectonic and petrological constraints from internal zones. PhD thesis, Universite Paris, France
- Richards, J. P., and Sholeh, A., 2016. The Tethyan tectonic history and Cu-Au metallogeny of Iran. *Tectonics and Metallogeny of the Tethyan Orogenic Belt*. Society of Economic Geologists, Special Publication, 19: 193–212.
- Richards, J.P., Spell, T., Rameh, E., Raziq, A. Fletcher, T., 2012. High Sr/Y magmas reflect arc maturity, high magmatic water content, and porphyry Cu ± Mo ± Au potential: examples from the Tethyan arcs of central and eastern Iran and western Pakistan. *Economic Geology*, 107(2): 295–312.
- Roedder, E., 1984. *Fluid inclusions: Reviews in mineralogy*, Mineralogical Society of America, 644 pp.
- Shahab pour, J., 2015. *Economic Geology*. (In Persian).
- Shepherd, T.J., Rankin, A.H., Alderton, D.H.M, 1985. *A practical guide to fluid inclusion studies*, Blackie, Glasgow, 239 pp.
- Sillitoe, R.H., 2010. Porphyry copper systems. *Economic geology*, 105(1): 3–41.
- Simmons, S.F., Simpson, M.P., Mauk, J., 2000. The mineral products of boiling in the golden cross epithermal deposit, New Zealand Minerals and Mining Conference Proceedings, 209-216.
- Stampfli GM, Borel GD., 2002. The TRANSMED transects in space and time: constraints on the paleotectonic evolution of the Mediterranean domain. In: Cavazza W, Roure F, Spakman W, Stampfli GM, Ziegler P (eds) *The TRANSMED Atlas: the Mediterranean region from crust to mantle*. Springer, Berlin, pp 53–80
- Stocklin, J., 1968. Structural history and tectonics of Iran: a review. *American Association of Petroleum Geologists Bulletin*, 52: 1229–1258.
- Stocklin, J., Nabavi, M.H., 1973. Tectonic map of Iran. Geological Survey of Iran, scale 1:2500000.
- Tarkian, M., Lotfi, M., Baumann, A., 1983. Tectonic, magmatism and the formation of mineral deposits in the central Lut, east Iran. *Geological Survey of Iran, geodynamic project (geotraverse) in Iran*, 51: 357–383.
- Tirrul, R., Bell, I.R., Griffis, R.J., Camp, V.E., 1983. The Sistan suture zone of eastern Iran. *Geological Society of America Bulletin*, 94: 134–156.
- Touret J, Dietvorst P., 1983. Fluid inclusions in high-grade anatectic metamorphites. *J Geol Soc (Lond)* 140:635–649
- Ulrich, T., Günther, D., Heinrich, C.A., 2001. The evolution of a porphyry Cu-Au deposit based on LA-ICP-MS

- analyses of fluid inclusions: Bajo de la Alumbrera, Argentina. *Economic Geology*, 96: 1743–1774.
- Ulrich, T., Heinrich, C.A., 2001. Geology and alteration geochemistry of the porphyry Cu-Au deposit at Bajo de La Alumbrera Argentina, *Economic Geology*, 96: 1719–1742.
- Van den Kerkhof, A.M., Hein, U.F., 2001. Fluid inclusion petrography. *Lithos*, 55: 27–47.
- Wilkinson, J.J., 2001. Fluid inclusions in hydrothermal ore deposit, *Lithos*, 55: 229–272.
- Zhang Y, Frantz JD .,1987. Determination of the homogenization temperatures and densities of supercritical fluids in the system NaCl–KCl–CaCl₂–H₂O using synthetic fluid inclusions. *Chem Geol* 64: 335–350